Massive Stars Near and Far
Proceedings IAU Symposium No. 361, 2024
J. Mackey, J. S. Vink, & N. St-Louis, eds.
doi:10.1017/S1743921322003404

X-raying massive stars and their feedback near and far

Lidia Oskinova

Institute for Physics and Astronomy, University Potsdam, D-14476 Potsdam, Germany
email: lida@astro.physik.uni-potsdam.de

Abstract. Massive stars emit X-rays. Despite modest X-ray luminosities of single hot massive stars, the ongoing large observing campaigns combining X-ray and UV spectroscopy provide a tomographic view of stellar winds. It is now established that X-ray radiation is modulated with stellar rotation and shows the same period as discrete absorption components (DACs) in the UV resonance lines. The latter are associated with corotating interaction regions (CIRs) in stellar winds, therefore the mechanisms responsible for generation of X-rays and CIRs appear to be physically linked. Binary massive stars with accreting compact companions – high-mass X-ray binaries (HMXBs) – are routinely observed by modern X-ray observatories at Mpc distances. Joint observations in X-ray and UV allow to determine realistic properties of these systems. The brightest sources among HMXBs are ultraluminous X-ray sources (ULXs). Their powerful radiation is an important source of stellar feedback. HMXBs are the products of massive binary evolution and are typically found in the vicinity of young massive star clusters. The superstar clusters blow hot superbubbles which fill large areas in star-forming dwarf galaxies. Recent models show that X-ray emission from superbubbles is likely the dominant source of He II ionization in metal-poor star-forming dwarf galaxies. To conclude, X-ray observations provide an important window for studying massive stars and their feedback near and far.

Keywords. X-rays: stars, X-rays: binaries, X-rays: ISM, galaxies: star clusters

1. Introduction

Since the first discovery of X-rays from sources outside of the Solar System exactly sixty years ago (Giacconi et al. 1962), X-ray observations remain at the frontiers of space observational astronomy. Among currently operating X-ray telescopes, two observatories are of special importance for studies of massive stars. The NASA's *Chandra* X-ray observatory provides an unprecedented sub-arcsecond angular resolution, as well as possibilities for low- and high-resolution X-ray spectroscopy. The ESA's X-ray Multi-Mirror Mission (*XMM-Newton*) is the largest X-ray telescope operating simultaneously all its instruments, including two high-resolution X-ray spectrographs. *Chandra* and *XMM-Newton* have similar passband ($1.2 - 120$ Å). Data obtained by these telescopes during more than 20 yr of operations are accumulated in the most recent *XMM-Newton* and *Chandra* catalogs – 4XMM-DR11 and CSC 2.0. The median X-ray flux of objects in these catalogs is $F_{\rm X} \sim 10^{-14}\,{\rm erg\,s^{-1}\,cm^{-2}}$ in the $0.3 - 7.0$ keV band (for comparison, the most sensitive *Chandra* observations reach a point source sensitivity $\sim 10^{-18}\,{\rm erg\,s^{-1}\,cm^{-2}}$).

Distances at which telescopes detect stars chiefly depend on the stellar X-ray luminosity and the intervening absorbing column. The typical X-ray luminosity of an O-type supergiant is $\sim 10^{33}$ erg s^{-1} (Nebot Gómez-Morán & Oskinova 2018) – therefore these objects could be detected with median length exposures within 30 kpc. Colliding wind binaries have an order of magnitude higher X-ray luminosities (Rauw & Nazé 2016),

and a higher than usual X-ray luminosity of a massive star is a reliable indicator of its binarity (Oskinova 2016). On the other hand, normal or low X-ray luminosity does not rule out that a massive star is a binary – enhanced X-ray luminosity is not a necessary attribute of massive binaries (Oskinova 2005, Nazé 2009). By now we know that all types of single hot massive stars, except of WC stars and LBVs, are X-ray sources. The X-ray loud WC stars and LBVs are colliding wind binaries (Oskinova et al. 2003, Nazé et al. 2012).

Massive stars which have a relativistic companion, a neutron star or a black hole, accreting stellar matter are called high-mass X-ray binaries (HMXBs). Typically, X-ray luminosities of persistent HMXBs are $> 10^{35}\,\mathrm{erg\,s^{-1}}$ while their X-ray spectra are hard. This allows easy detection of HMXBs at distances up to $\sim 300\,\mathrm{kpc}$. The hardness of spectra drastically reduces the influence of the interstellar absorption and allows to observe HMXBs across the Galaxy. In fact, the census of persistent HMXBs is nearly complete in the Galaxy and in the Magellanic Clouds (Liu et al. 2006, Krivonos et al. 2012, Haberl & Sturm 2016). The most luminous sources among the HMXB population belong to the class of ultraluminous X-ray sources (ULXs) with $L_{\mathrm{X}} > 10^{39}\,\mathrm{erg\,s^{-1}}$ (Walton et al. 2022). These enigmatic objects are easily detectable within $\sim 3\,\mathrm{Mpc}$.

2. X-rays from single massive stars are modulated with stellar rotation

X-ray spectroscopic diagnostics revealed that in single massive stars X-rays are generated close to photosphere in hot plasma expanding with velocities similar to the general cool wind velocity (Waldron & Cassinelli 2007). X-rays suffer absorption in the cool wind but wind clumping allows more radiation to escape than would be possible if winds were smooth (Oskinova et al. 2006). Observations of HMXBs allow to directly detect spectroscopic signatures of clumps which are optically thick for X-rays (Goldstein et al. 2004, Oskinova et al. 2012, Martínez-Chicharro et al. 2021). At the same time, dedicated searches using excellent data ruled out the presence of stochastic variability which could be linked to strong shocks in stellar winds (Nazé et al. 2013, Nichols et al. 2015).

There is firm evidence that X-rays from single O and WR stars are variable at $\sim 10-20\%$ level on the rotational time scale (Oskinova et al. 2001, Ignace et al. 2013, Massa et al. 2014). Nichols et al. (2021) found that the X-ray flux of the prototypical O-type supergiant ζ Puppis (O4I) is modulated with $P = 1.78\,\mathrm{d}$, i. e. the same period as observed in the broad-band optical photometric light-curve albeit in anti-phase with it.

The association of X-rays with the large scale structures in rotating star winds – corotating interaction regions (CIRs) – has been long predicted (Mullan 1984). The signatures of the CIRs are observed as discrete absorption components (DACs) in the UV resonance lines which originate in stellar winds (Prinja & Howarth 1986, Hamann et al. 2001). To obtain a tomographic view of stellar winds and uncover links between the CIRs and X-ray emission we initiated observing campaigns using the *HST* STIS UV spectrograph and the *XMM-Newton* X-ray telescope. We selected two fast rotating single O-type stars: ξ Per (O7.5III) and ζ Oph (O9.2IV). These objects have different wind strengths, with ξ Per's wind being more dense than ζ Oph's wind, and also different pulsation and rotation periods.

Massa et al. (2019) presented the results of joint *XMM-Newton* and *HST* observations of ξ Per. The detailed study of the UV spectral variability revealed that it remains consistent for at least 22 years elapsed since the previous UV spectral study of this object. The DACs recurrence time, 2.1 d, remained stable. The X-ray variability period is the same as the DACs period, however we established that there is a phase shift between normalized X-ray and the UV wind line fluxes.

https://doi.org/10.1017/S1743921322003404 Published online by Cambridge University Press

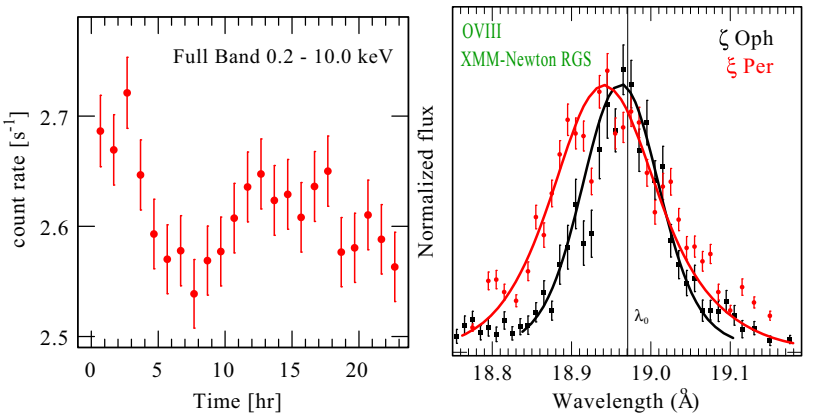

Figure 1. *Left: XMM-Newton* EPIC pn background-subtracted X-ray light curve of ζ Oph in the $0.2-10.0$ keV band. The data are binned to 30 min. The horizontal axis denotes the time after the beginning of the observation in hours. The vertical axis shows the count rate as measured by the EPIC pn camera. The error bars (1σ) correspond to the combination of the error in the source counts and the background counts. *Right: XMM-Newton* RGS spectra of the resonance line O VIII λ18.97 Å obtained during the observations of ξ Per (red error bars) and ζ Oph (black error bars). The solid lines show corresponding line profiles predicted by our clumped wind models (Oskinova et al. 2006).

Similar results are found from the analysis of the recent *XMM-Newton* observations of ζ Oph which covered the full rotational period of the star, $P_{\rm rot} \approx 15.28$ hr, as well as its DACs recurrence period, $P_{\rm UV} \approx 20.8$ hr (Howarth et al. 1993). As illustrated in Fig. 1, the X-ray light curve is modulated with rotational period. The analysis of *HST* spectroscopic observations which are nearly simultaneous with the X-ray observations is ongoing.

Thus, the current data point out that the generation of X-rays in massive stars is linked with rotation and is associated with large scale wind structures. Furthermore, the presence of the CIRs was invoked by Bozzo et al. (2017) to explain the observed super-orbital modulation of the X-ray flux in supergiant HMXBs.

3. Hot winds as an explanation of the weak-wind problem

Figure 1 shows the O VIII λ18.97 Å resonance line in the spectra of ξ Per and ζ Oph. The strong absorption of X-rays in the dense wind of ξ Per leads to the line blue-shift (Oskinova et al. 2006). In contrast, the wind of ζ Oph is essentially transparent for emergent X-rays in agreement with the low mass-loss rates inferred from the analyses of UV spectra (Martins et al. 2005). As a result, the observed X-ray emission line is not blue-shifted.

X-rays associated with hot plasma distributed in stellar winds have long been invoked as a promising solution of the so-called *weak wind problem* (Cassinelli et al. 1994, Martins et al. 2005, Lagae et al. 2021). Lucy (2012) suggested that in the late-type O-dwarfs the bulk of the wind is hot, with temperatures of a few MK. The cool radiatively driven gas is confined to dense clumps. Further out in the wind, these cool clumps are destroyed by heat conduction, and the outflow is dominated by a hot thermal wind which reaches a supersonic terminal velocities.

Independently, similar solution to the weak-wind problem was proposed by Huenemoerder et al. (2012) based on the empiric study of the high-resolution X-ray spectra of late O-type dwarfs, μ Col and σ Ori AB. It was shown that the emission measure of the X-ray emitting plasma is much larger than emission measure of the cool wind. Huenemoerder et al. (2012) proposed that the weak-wind problem is resolved when the

https://doi.org/10.1017/S1743921322003404 Published online by Cambridge University Press

hot dominant component of the wind is accounted for in the total mass-loss rate budget. It was suggested that "the wind is not weak, but it is hot and its bulk is only detectable in X-rays." The preliminary results of our ongoing study of another O-dwarf, ζ Oph, corroborate this conclusion.

4. High-mass X-ray binaries and ULXs

Traditionally, the focus in studies of HMXBs lies on the analysis of their X-ray spectra and light-curves. However, recent work shows that detailed modeling of donor star spectra in optical and UV is needed to obtain realistic physical description of these systems.

The HMXBs with OB supergiant donor stars are classified in two groups according to their X-ray properties: persistent sources and supergiant fast X-ray transients (SFXTs, Martínez-Núñez et al. 2017). It has been suggested that this dichotomy depends on the characteristics of stellar winds, such as enhanced clumping or weaker winds in SFXTs compared to the persistent sources. Hainich et al. (2020) analyzed stellar and wind parameters of six HMXBs using UV spectra obtained with the *HST*. This thorough study showed that winds of donor stars in SFXTs and persistent HMXBs are similar. Recently, (Sidoli et al. 2021) detected intrinsic X-ray emission from the O-type donor in a quiescent SFXT, further confirming that winds of donors in SFXTs are not special. The SFXT phenomenon could be explained by interactions between the neutron star's magnetic field, its spin, and the dynamics of donor star wind (Bozzo et al. 2008, Shakura et al. 2014, Bozzo et al. 2016). Grids of spectral models for OB stars at different metallicities can be used for analyzes of donor stars in HMXBs (Hainich et al. 2019).

HMXBs and ULXs are important sources of feedback (Lebouteiller et al. 2017, Sazonov & Khabibullin 2018, Schaerer et al. 2019). Oskinova et al. (2019) discovered three ULXs in the metal-poor galaxy ESO 338 and suggested that, in order to adequately model stellar feedback in this and similar low-metallicity dwarf galaxies, X-rays have to be taken into account.

5. X-ray emission from hot superbubbles explain nebular He II emission in metal-poor dwarf galaxies

Star-forming galaxies are filled by diffuse X-rays produced by a few MK hot gas (e.g. Martin 1996, Tenorio-Tagle et al. 2006, Danehkar et al. 2021). Observations establish that its X-ray luminosity is proportional to the star-formation rate (SFR) of the host galaxy (Smith et al. 2019, Mineo et al. 2012, Lehmer et al. 2022). Oskinova & Schaerer (2022) suggest that the nebular He II emission observed in dwarf galaxies can be explained by X-rays from superbubbles blown up by cluster winds of superstar clusters with $M_{\rm cl} > 10^5\,M_\odot$. The kinetic energy feedback of massive stars increases as star clusters evolve, and reaches its maximum in a few Myr old clusters (Oskinova 2005). Initially, the energy input is dominated by stellar winds, while later on it gradually increases due to the input from core-collapse supernovae.

The temperature of superbubbles scales with input kinetic energy. Because at lower metallicities stellar winds are weaker, superbubble temperatures are also lower. Therefore, at low metallicity, the bulk of the X-rays emerging from superbubbles has energies close to the He II ionization edge.

In order to estimate the He II ionizing power of the whole ensemble of young star clusters in a star-forming galaxy, Oskinova & Schaerer (2022) employed an empirical correlation between the cluster formation rate and SFR in galaxies. It was shown that X-ray luminosity of hot diffuse gas in a galaxy is proportional to its SFR $[M_\odot\,{\rm yr}^{-1}]$ as $\log L_{\rm X} \approx \log {\rm SFR} + 39.6\,[{\rm erg\,s}^{-1}]$, i.e. similar to observations (Lehmer et al. 2022). Hence, according to this model, the observed prevalence of He II nebulae in low-Z galaxies is

https://doi.org/10.1017/S1743921322003404 Published online by Cambridge University Press

Table 1. He II ionizing photon rate in WR stars and hot superbubbles (SBB) with $L_X(\mathrm{SBB}) = 10^{40}\,\mathrm{erg\,s^{-1}}$. The metallicity is $Z = 0.07 Z_\odot$.

Object	**Model***	**Temperature**	$\log Q(\mathrm{He}^+)$ $[\mathrm{s}^{-1}]$
WNE star	WNE-2014 model 16-14	$T_* = 141\,\mathrm{kK}$	48.2
WNL star	WNL-H60-20	$T_* = 110\,\mathrm{kK}$	47.8
WC star	WC-19-18	$T_* = 200\,\mathrm{kK}$	48.5
WNE star	WNE-18-13	$T_* = 178\,\mathrm{kK}$	48.4
WNL star	WNL-H60-14-06	$T_* = 112\,\mathrm{kK}$	47.7
SBB	*apec*	$kT = 0.5\,\mathrm{keV}$	49.7
SBB	*apec*	$kT = 0.2\,\mathrm{keV}$	50.2
SBB	*apec*	$kT = 0.1\,\mathrm{keV}$	51.0

(*) For WR stars, the model number is according to the PoWR model grid accessible at www.astro.physik.uni-potsdam.de/PoWR.

due to the combination of (1) lower temperature of superbubbles, (2) the linear scaling between the X-ray output of star clusters and the SFR of their host galaxy.

Besides superbubbles, WR stars also contribute to the He II ionizing flux (Table 1). The Oskinova & Schaerer (2022) model links star and cluster formation with stellar evolution and feedback. Consistent modeling of galaxies exhibiting He II nebula emission is the next required step in understanding stellar feedback at low metallicity.

Acknowledgements

This work would have been impossible without my co-authors and collaborators. Special thanks and appreciation of their valuable work are to the current PhD students – Matthew Rickard, Timothy Parsons, Sabela Reyero, and Daniel Pauli.

References

Bozzo, E., Falanga, M., & Stella, L. 2008, ApJ, 683, 1031
Bozzo, E., Oskinova, L., Feldmeier, A., & Falanga, M. 2016, A&A, 589, A102
Bozzo, E., Oskinova, L., Lobel, A., & Hamann, W. R. 2017, A&A, 606, L10
Cassinelli, J. P., Cohen, D. H., Macfarlane, J. J., Sanders, W. T., & Welsh, B. Y. 1994, ApJ, 421, 705
Danehkar, A., Oey, M. S., & Gray, W. J. 2021, ApJ, 921, 91
Giacconi, R., Gursky, H., Paolini, F. R., & Rossi, B. B. 1962, Physical Review Letters, 9, 439
Goldstein, G., Huenemoerder, D. P., & Blank, D. 2004, AJ, 127, 2310
Haberl, F., & Sturm, R. 2016, A&A, 586, A81
Hainich, R., Ramachandran, V., Shenar, T., Sander, A. A. C., Todt, H., Gruner, D., Oskinova, L. M., & Hamann, W. R. 2019, A&A, 621, A85
Hainich, R., et al. 2020, A&A, 634, A49
Hamann, W. R., Brown, J. C., Feldmeier, A., & Oskinova, L. M. 2001, A&A, 378, 946
Howarth, I. D., et al. 1993, ApJ, 417, 338
Huenemoerder, D. P., Oskinova, L. M., Ignace, R., Waldron, W. L., Todt, H., Hamaguchi, K., & Kitamoto, S. 2012, ApJL, 756, L34
Ignace, R., Gayley, K. G., Hamann, W. R., Huenemoerder, D. P., Oskinova, L. M., Pollock, A. M. T., & McFall, M. 2013, ApJ, 775, 29
Krivonos, R., Tsygankov, S., Lutovinov, A., Revnivtsev, M., Churazov, E., & Sunyaev, R. 2012, A&A, 545, A27
Lagae, C., Driessen, F. A., Hennicker, L., Kee, N. D., & Sundqvist, J. O. 2021, A&A, 648, A94
Lebouteiller, V., et al. 2017, A&A, 602, A45
Lehmer, B. D., Eufrasio, R. T., Basu-Zych, A., Garofali, K., Gilbertson, W., Mesinger, A., & Yukita, M. 2022, ApJ, 930, 135
Liu, Q. Z., van Paradijs, J., & van den Heuvel, E. P. J. 2006, A&A, 455, 1165
Lucy, L. B. 2012, A&A, 544, A120

https://doi.org/10.1017/S1743921322003404 Published online by Cambridge University Press

Martin, C. L. 1996, ApJ, 465, 680
Martínez-Chicharro, M., et al. 2021, MNRAS, 501, 5646
Martínez-Núñez, S., et al. 2017, Space Science Reviews, 212, 59
Martins, F., Schaerer, D., Hillier, D. J., Meynadier, F., Heydari-Malayeri, M., & Walborn, N. R. 2005, A&A, 441, 735
Massa, D., Oskinova, L., Fullerton, A. W., Prinja, R. K., Bohlender, D. A., Morrison, N. D., Blake, M., & Pych, W. 2014, MNRAS, 441, 2173
Massa, D., Oskinova, L., Prinja, R., & Ignace, R. 2019, ApJ, 873, 81
Mineo, S., Gilfanov, M., & Sunyaev, R. 2012, MNRAS, 426, 1870
Mullan, D. J. 1984, ApJ, 283, 303
Nazé, Y. 2009, A&A, 506, 1055
Nazé, Y., Oskinova, L. M., & Gosset, E. 2013, ApJ, 763, 143
Nazé, Y., Rauw, G., & Hutsemékers, D. 2012, A&A, 538, A47
Nebot Gómez-Morán, A., & Oskinova, L. M. 2018, A&A, 620, A89
Nichols, J., et al. 2015, ApJ, 809, 133
Nichols, J. S., et al. 2021, ApJ, 906, 89
Oskinova, L. M. 2005, MNRAS, 361, 679
—. 2016, Advances in Space Research, 58, 739
Oskinova, L. M., Bik, A., Mas-Hesse, J. M., Hayes, M., Adamo, A., Östlin, G., Fürst, F., & Otí-Floranes, H. 2019, A&A, 627, A63
Oskinova, L. M., Clarke, D., & Pollock, A. M. T. 2001, A&A, 378, L21
Oskinova, L. M., Feldmeier, A., & Hamann, W. R. 2006, MNRAS, 372, 313
Oskinova, L. M., Feldmeier, A., & Kretschmar, P. 2012, MNRAS, 421, 2820
Oskinova, L. M., Ignace, R., Hamann, W. R., Pollock, A. M. T., & Brown, J. C. 2003, A&A, 402, 755
Oskinova, L. M., & Schaerer, D. 2022, A&A, 661, A67
Prinja, R. K., & Howarth, I. D. 1986, ApJS, 61, 357
Rauw, G., & Nazé, Y. 2016, Advances in Space Research, 58, 761
Sazonov, S., & Khabibullin, I. 2018, MNRAS, 476, 2530
Schaerer, D., Fragos, T., & Izotov, Y. I. 2019, A&A, 622, L10
Shakura, N., Postnov, K., Sidoli, L., & Paizis, A. 2014, MNRAS, 442, 2325
Sidoli, L., Postnov, K., Oskinova, L., Esposito, P., De Luca, A., Marelli, M., & Salvaterra, R. 2021, A&A, 654, A131
Smith, B. J., Wagstaff, P., Struck, C., Soria, R., Dunn, B., Swartz, D., & Giroux, M. L. 2019, AJ, 158, 169
Tenorio-Tagle, G., Muñoz-Tuñón, C., Pérez, E., Silich, S., & Telles, E. 2006, ApJ, 643, 186
Waldron, W. L., & Cassinelli, J. P. 2007, ApJ, 668, 456
Walton, D. J., Mackenzie, A. D. A., Gully, H., Patel, N. R., Roberts, T. P., Earnshaw, H. P., & Mateos, S. 2022, MNRAS, 509, 1587